11th World Congress on Computational Mechanics (WCCM XI)
5th European Conference on Computational Mechanics (ECCM V)
6th European Conference on Computational Fluid Dynamics (ECFD VI)
E. Oñate, J. Oliver and A. Huerta (Eds)

NUMERICAL SIMULATION OF DAMAGE AND FAILURE BEHAVIOR OF BIAXIALLY LOADED SPECIMENS

DANIEL BRENNER, STEFFEN GERKE AND MICHAEL BRÜNIG

Institut für Mechanik und Statik
Universität der Bundeswehr München
Werner-Heisenberg-Weg 39, 85577 Neubiberg, Germany
e-mail: daniel.brenner@unibw.de, www.unibw.de/baumechanik

Key Words: *Damage and failure, Biaxially loaded specimens, Stress-state-dependence, Ductile metals.*

Abstract. The paper deals with the effect of stress state on damage and failure behavior of ductile metals. Within the general framework of continuum thermodynamics of irreversible processes an anisotropic damage and failure model as well as its numerical implementation are discussed. The approach is based on the introduction of damaged and fictitious undamaged configurations and takes into account kinematic definition of damage tensors. Onset of plastic flow is characterized by a generalized hydrostatic-stress-dependent yield condition and a non-associated flow rule. Furthermore, a damage criterion formulated in stress space is proposed. It is based on series of experiments and corresponding numerical simulations as well as on various numerical calculations on the micro-level. Different branches of the damage criterion depending on stress triaxiality and Lode parameter are considered. To be able to take into account a wide range of different stress states new experiments with two-dimensionally loaded specimens have been developed. Numerical simulations of these shear-tension and shear-compression tests permit validation of stress-state-dependent functions for the damage criteria and damage evolution laws. In addition, comparison of experimental and numerical results are used to identify corresponding constitutive parameters.

1 INTRODUCTION

Modeling and numerical simulation of inelastic behaviour, damage and failure of materials used in different engineering disciplines is an important topic in solid, structural and computational mechanics. Based on many experimental observations it is well known that moderate and large inelastic deformations caused by complex static and dynamic loadings of ductile metals are accompanied by damage and local failure mechanisms acting on different scales leading to macro-failure of structural elements. In particular, under tension dominated loading conditions with high positive stress triaxialities damage in ductile metals is mainly caused by nucleation, growth and coalescence of micro-voids. However, during shear and compression tests with small positive or negative stress triaxialities evolution and growth of micro-shear-cracks are the prevailing damage and failure mechanisms on the micro-scale. In

addition, between these regions of stress triaxialities there is a zone with combination of the two basic mechanisms discussed above with simultaneous formation and growth of micro-voids and micro-shear-cracks [1, 2, 7, 8]. Furthermore, it has been observed that no damage occurs in material samples under high compression loading [3]. Therefore, it is important to analyse and to understand these stress-state-dependent damage and failure processes as well as the corresponding mechanisms acting on different scales to be able to propose and to develop a realistic phenomenological model as well as an accurate and efficient numerical approach.

To be able to get more information on stress-state-dependent damage and failure behavior uniaxial tension tests with un-notched and differently pre-notched specimens and corresponding numerical simulations have been performed [2, 4, 7, 8, 12, 13]. However, these experiments only cover a small region of positive stress triaxialities between 0.33 and 0.60. Thus, new geometries of specimens tested under uniaxial tension have been designed to analyse stress states with nearly zero stress triaxialities [2, 8, 11, 13]. Furthermore, for other regions of stress triaxialities butterfly specimens have been developed [14]. Using special experimental equipment these specimens can be tested in different directions. Corresponding numerical simulations have shown that these tests lead to stress triaxialities between -0.33 and 0.60.

On the numerical side, efficient, robust and accurate numerical algorithms are required to be able to solve complex boundary-value problems. Integration of the constitutive rate equations is often performed using an extension of the well-known radial return technique [10, 15]. Alternatively, a generalized inelastic predictor-elastic corrector technique has been proposed which yields accurate solutions for inelastic materials even when large time steps are taken into account [6].

In the present paper numerical simulations of new experiments with biaxially loaded specimens will be presented covering a wide range of stress states corresponding to different damage and failure mechanisms acting on the micro-scale. The geometry of the specimens allows combination of shear-tension and shear-compression mechanisms with various ratios of respective loads. Numerical analyses of these tests will show that they cover a wide range of stress triaxialities with different Lode parameters. These simulations allow validation of stress-state-dependent functions for damage and failure criteria as well as damage evolution laws.

2 CONTINUUM DAMAGE MODEL

The continuum damage model presented by [5] is used to predict the elastic-plastic deformations including damage. It takes into account information of the mechanisms of individual micro-defects and their interactions detected by numerical calculations on the micro-level [9]. The phenomenological approach is based on the consideration of damaged and fictitious undamaged configurations. The kinematics leads to the additive decomposition of the strain rate tensor into elastic, plastic and damage parts.

Constitutive equations modeling the elastic-plastic behavior of the undamaged matrix material are formulated with respect to the undamaged configurations. The elastic behavior is represented by Hooke’s law and onset and continuation of plastic yielding of the considered aluminum alloy is modeled by the yield condition

$$f^{\mathrm{pl}} = \sqrt{\bar{J}_2} - c\left(1 - \frac{a}{c}\bar{I}_1\right) = 0 \tag{1}$$

where $\bar{I}_1$ and $\bar{J}_2$ are the first and the second deviatoric invariants of the effective stress tensor $\bar{\mathbf{T}}$ (referred to the undamaged configurations), c denotes the strength coefficient and a represents the hydrostatic stress coefficient of the matrix material. In elastic-plastically deformed and damaged metals irreversible volumetric strain rates are mainly caused by damage and, in comparison, volumetric plastic strain rates are negligibly small. Thus, the isochoric effective plastic strain rate

$$\dot{\mathbf{H}}^{\mathrm{pl}} = \dot{\gamma}\frac{1}{\sqrt{2\bar{J}_2}}\mathrm{dev}\bar{\mathbf{T}} \tag{2}$$

describes the evolution of plastic deformations in an accurate manner where the non-negative scalar-valued factor $\dot{\gamma}$ represents the equivalent plastic strain rate measure used in the present phenomenological constitutive approach.

Furthermore, corresponding anisotropically damaged configurations are considered to formulate the constitutive equations characterizing the elastic and damage behavior of the damaged aggregate [5]. In particular, the generalized elastic-damage constitutive law is a function of elastic and damage strain tensors. This allows simulation of deterioration of elastic material properties caused by formation and growth of micro-defects. In addition, onset and continuation of damage during further loading of material samples is governed by a stress-state-dependent damage criterion. In this context, different damage and failure mechanisms acting on the micro-level are taken into account [2, 7, 9] leading to consideration of a wide range of stress triaxialities with different branches: damage and failure are a consequence of nucleation and growth of nearly spherical micro-voids for large positive stress triaxialities, by formation and growth of micro-shear-cracks in the negative stress triaxiality regime and by combination of these basic mechanisms acting on the micro-level for low positive stress triaxialities. Furthermore, for stress states with remarkable hydrostatic pressure a cut-off value has been proposed below which damage and failure do not occur. This stress-state-dependent concept is taken into account in the present investigation and will be generalized by additional consideration of the Lode parameter.

Thus, the onset and continuation of continuum damage is assumed to be governed by the damage criterion

$$f^{\mathrm{da}} = \alpha I_1 + \beta\sqrt{J_2} - \sigma = 0 \tag{3}$$

where σ is the damage threshold and α and β represent the stress-state-dependent damage mode parameters. These variables correspond to the different branches discussed above and depend on the stress triaxiality

$$\eta = \sigma_{\mathrm{m}} / \sigma_{\mathrm{eq}} = I_1 / \left(3\sqrt{3J_2}\right) \tag{4}$$

defined as the ratio of the mean stress σ_m and the von Mises equivalent stress σ_{eq} as well as on the Lode parameter

$$\omega = \frac{2\tilde{T}_2 - \tilde{T}_1 - \tilde{T}_3}{\tilde{T}_1 - \tilde{T}_3} \quad \text{with} \quad \tilde{T}_1 \geq \tilde{T}_2 \geq \tilde{T}_3 \tag{5}$$

expressed in terms of the principal Kirchhoff stress components $\tilde{T}_1$, $\tilde{T}_2$ and $\tilde{T}_3$ with respect to the damaged configurations.

The increase in macroscopic strains caused by formation and growth of micro-defects leading to anisotropic damage behavior is modeled by the damage rule

$$\dot{\mathbf{H}}^{da} = \dot{\mu}\left(\bar{\alpha}\frac{1}{\sqrt{3}}\mathbf{1} + \bar{\beta}\mathbf{N} + \bar{\delta}\mathbf{M} \right) \quad . \tag{6}$$

In Eq. (6) $\bar{\alpha}$, $\bar{\beta}$ and $\bar{\delta}$ are stress-state-dependent kinematic variables and $\dot{\mu}$ represents the rate of the equivalent damage strain. In addition, $\mathbf{N} = \left(\sqrt{2J_2}\right)^{-1} \mathrm{dev}\tilde{\mathbf{T}}$ and $\mathbf{M} = \left(\left\|\mathrm{dev}\tilde{\mathbf{S}}\right\|\right)^{-1} \mathrm{dev}\tilde{\mathbf{S}}$ are normalized deviatoric stress tensors where $\tilde{\mathbf{T}}$ denotes the stress tensor work-conjugate to the damage strain rate (6) and

$$\mathrm{dev}\tilde{\mathbf{S}} = \mathrm{dev}\tilde{\mathbf{T}}\mathrm{dev}\tilde{\mathbf{T}} - \frac{2}{3}J_2\mathbf{1} \, . \tag{7}$$

It should be noted that it was not possible to identify all parameters appearing in the constitutive equations and their stress-state-dependence only by tension tests and, therefore, three-dimensional unit cell model calculations have been performed covering a wide range of stress triaxialities and Lode parameters [9]. Based on these numerical results the stress-state-dependent parameters α and β (Eq. (3)) as well as $\bar{\alpha}$, $\bar{\beta}$ and $\bar{\delta}$ (Eq. (6)) have been identified for an aluminum alloy. However, the respective stress-state-dependent functions of these parameters are only based on numerical calculations on the micro-level and, thus, series of new experiments with two-dimensionally loaded specimens and corresponding numerical simulations of these tests have been performed to be able to validate the stress-state-dependent damage criteria (3) and damage rules (6) or to propose simpler experimentally based functions as well as to identify further material parameters of the continuum model.

3 NUMERICAL ASPECTS

The constitutive rate equations have been numerically integrated using an extended version of the inelastic predictor-elastic corrector technique [6]. Corresponding tangent moduli have been developed leading to quadratic convergence of the solution of the system of nonlinear equations. The continuum approach has been implemented in the finite element program ANSYS as a user-defined material subroutine.

4 NUMERICAL SIMULATION OF 2D-EXPERIMENTS

Numerical simulations of experiments with uniaxially and biaxially loaded specimens have been performed to identify material parameters and stress-state-dependent functions of the continuum damage model. In particular, basic elastic-plastic material parameters are identified by analyzing uniaxial tension tests with unnotched flat specimens. Equivalent stress-equivalent strain curves are obtained from load-displacement curves as long as the uniaxial stress state is homogeneous in the central part of the specimen. For the investigated aluminum alloy fitting of experimental and numerical equivalent stress-equivalent strain curves leads to Young's modulus E = 65000 MPa and Poisson's ratio is taken to be ν = 0.3.

Furthermore, the power-law function for the equivalent stress

$$c = c_0 \left(\frac{H\gamma}{nc_0} + 1 \right)^n . \tag{8}$$

numerically simulates the work-hardening behavior of the ductile metal with the initial yield strength c_0 = 175 MPa, the hardening modulus H = 2100 MPa and the exponent n = 0.22.

Using these material data numerical simulations of biaxially loaded specimens tested in a 2D-tension/compression machine have been performed. Figure 1 shows the finite element mesh with three-dimensional discretization using 42248 eight-node solid185 elements. Remarkable refinement of the mesh is used in the central part of the specimen where a notch in thickness direction has been added. Due to the geometry of the specimen vertical loads will lead to shear mechanisms in the specimen's center whereas horizontal loads will lead to additional tension or compression modes. Thus, with simultaneous loading in vertical and horizontal direction it will be possible to get information of the effect of different stress states on inelastic deformation, damage and failure behavior. These tests with different positive and negative load ratios are a generalization of uniaxial experiments with this kind of specimens with subsequent shear and tension tests [11].

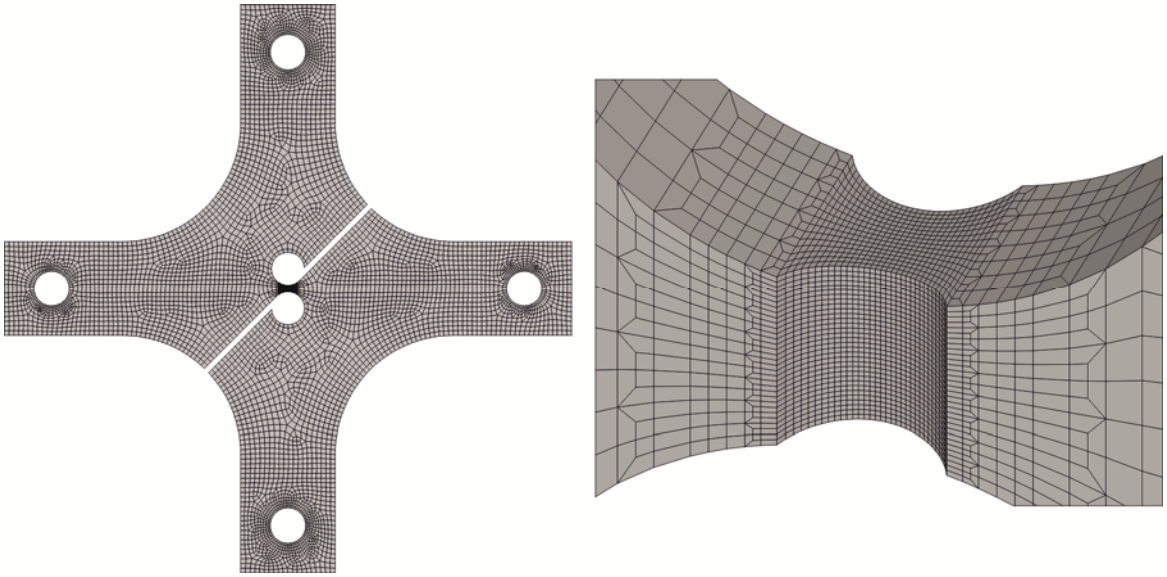

Figure 1: Finite element mesh

Results of the biaxial test with load ratio F_1:F_2 = 1:1 and of corresponding elastic-plastic numerical calculation are compared in Fig. 2. Experimental and numerically predicted load-displacement curves show good agreement and only deviation in the last part. This deviation is caused by the occurrence of damage in the experiment which was not taken into account in the numerical simulation. Thus, onset of deviation characterizes onset of damage in the specimen during this test. At this loading stage the stress state in the specimen's center is analyzed in detail to be able to study the influence of the stress state on the damage criterion (3).

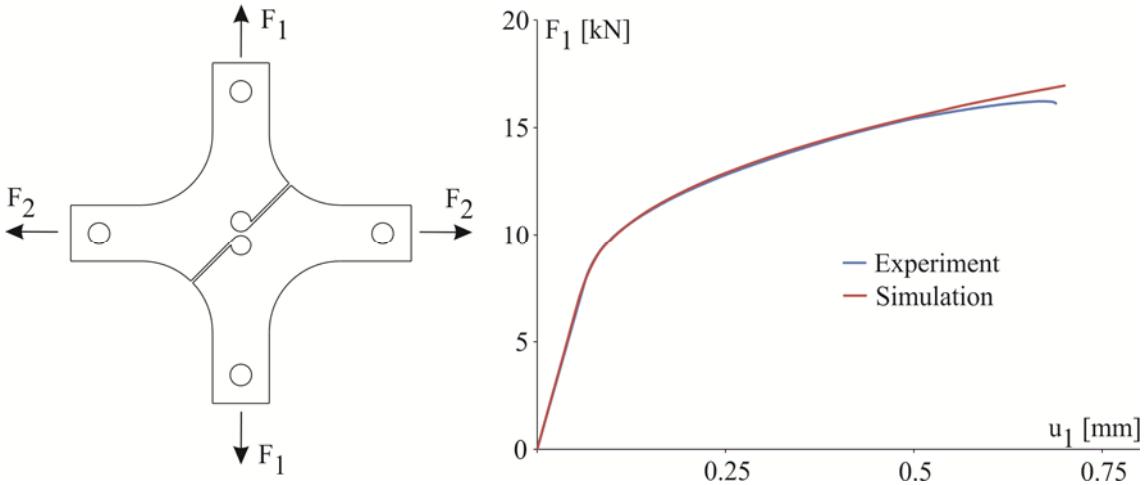

Figure 2: Biaxially loaded specimen and load-displacement curves

Distribution of the first and second deviatoric stress invariants, I_1 and $\sqrt{J_2}$, are shown in Fig. 3. In particular, maximum of the first stress invariant is numerically predicted on the boundaries of the notched part near the center of the specimen. In this part, also very high values of the second deviatoric stress invariant can be seen whereas maxima of $\sqrt{J_2}$ appear in the specimen's center. Thus, damage will start in the region with very high values of I_1 and $\sqrt{J_2}$.

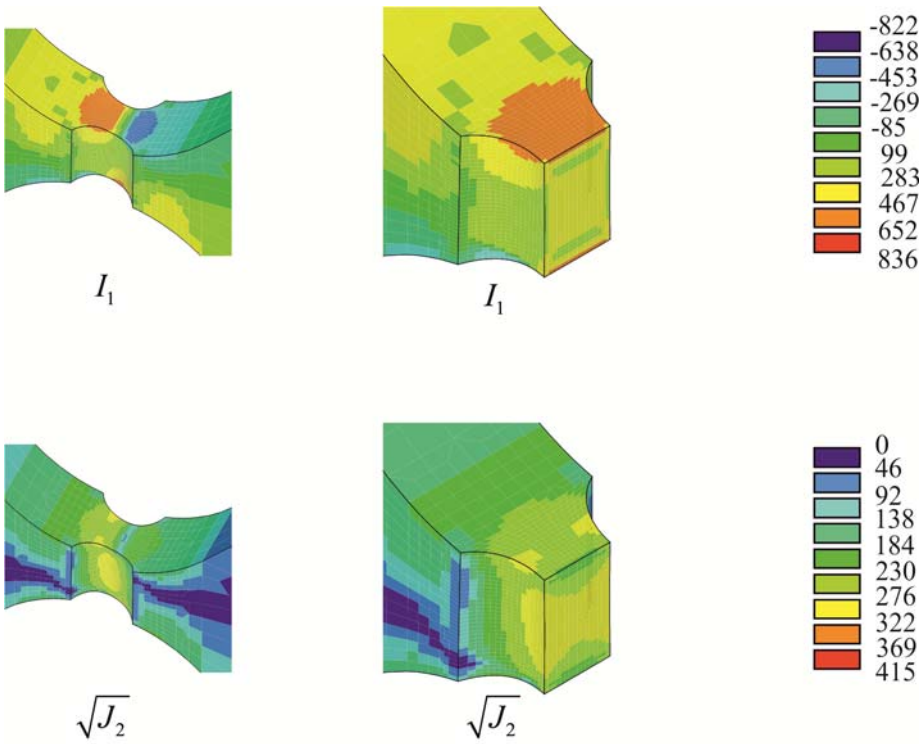

Figure 3: Distribution of the first and second deviatoric stress invariants

Different load ratios have remarkable effect on the stress states in the center of the specimen. For example, Fig. 4 shows the numerically predicted distribution of the stress triaxiality η in the specimen's center (vertical section) at onset of damage. In particular, in uniaxial tension loading (F_1:F_2 = 0:1) remarkable high stress triaxiality of η = 0.84 is numerically predicted in the midpoint of the specimen which will lead to void growth modes. This high stress triaxiality is a consequence of the notches in horizontal and thickness direction. On the other hand, nearly zero stress triaxiality exists when the specimen is only loaded by F_1 (F_1:F_2 =1:0). This will lead to formation of micro-shear-cracks. Additional forces F_2 in horizontal direction will lead to different stress triaxialities which are nearly constant over the central area shown in Fig. 2. The loading ratio F_1:F_2 =1:1 leads to η = 0.25, the ratio F_1:F_2 =1:0.5 to η = 0.14, and the ratio F_1:F_2 =1:-0.5 to η = -0.14 corresponding to different damage modes.

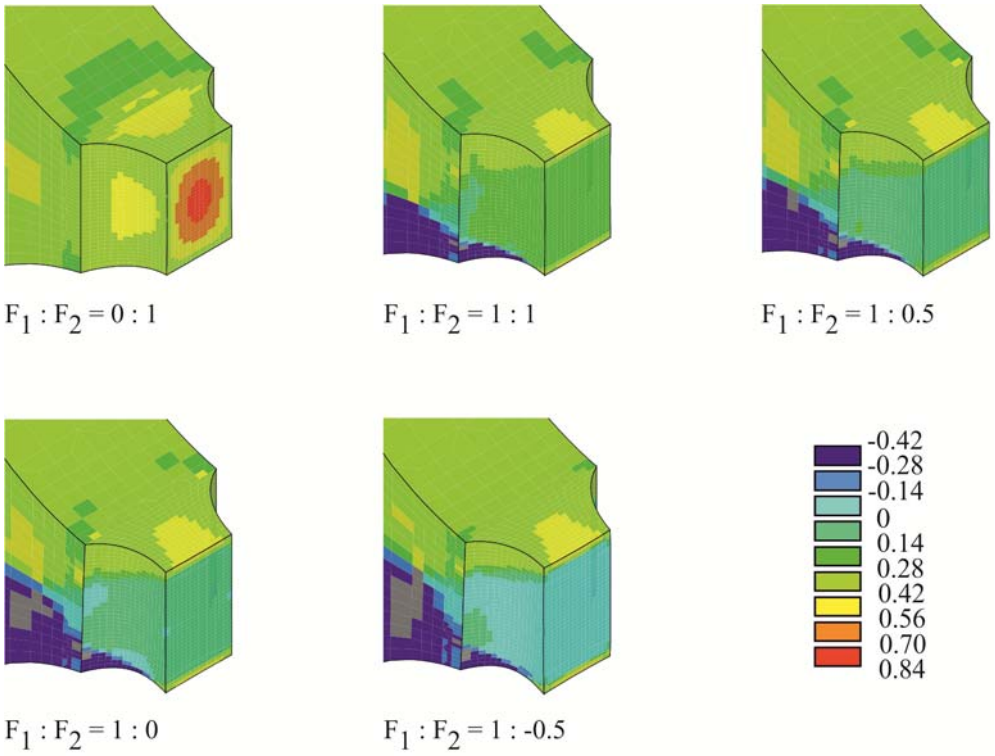

Figure 4: Distribution of the stress triaxiality η for different load ratios

Furthermore, Fig. 5 shows the distribution of the Lode parameter ω in the specimen's center at onset of damage for different loading ratios. For example, in uniaxial tension loading (F_1:F_2 = 0:1) the Lode parameter of ω = -1.0 is numerically predicted in the central cross section of the specimen. On the other hand, nearly zero Lode parameter exists in the shear mode regime when the specimen is only loaded by F_1 (F_1:F_2 =1:0). Additional forces F_2 in horizontal direction will lead to different Lode parameters which then become more

inhomogeneous over the cross section shown in Fig. 5. For example, the loading ratio F_1:F_2 =1:1 leads in this area to various Lode parameters between ω = -0.50 and ω = -0.10, the ratio F_1:F_2 =1:0.5 to nearly homogeneous ω = -0.10, and the ratio F_1:F_2 =1:-0.5 to inhomogeneous distribution up to ω = 0.20. These different stress states allow validation of the stress-state-dependent damage criterion based on series of numerical calculations on the micro-level [9].

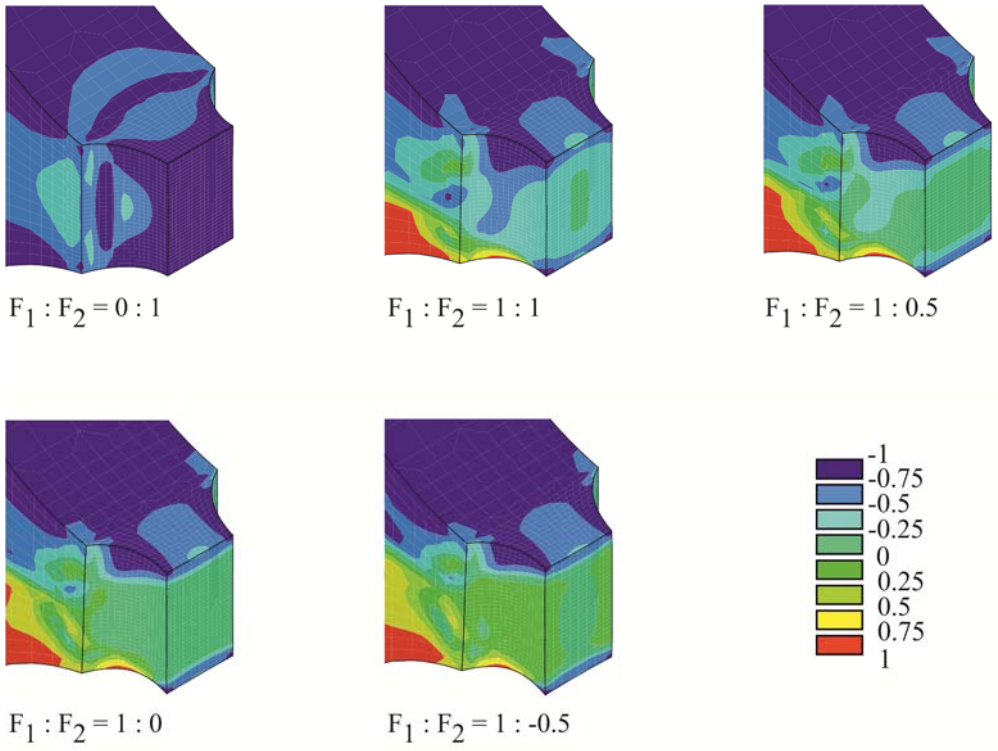

Figure 5: Distribution of the Lode parameter ω for different load ratios

5 CONCLUSIONS

A continuum damage model and corresponding numerical aspects have been discussed. Damage condition and damage evolution laws take into account the effect of stress state on damage and failure mechanisms acting on the micro-level. To be able to propose stress-state-dependent criteria numerical simulations of new 2D experiments with biaxially loaded specimens have been performed. It has been shown that a wide range of stress triaxialities and Lode parameters can be considered and their effect on onset and propagation of damage can be analyzed in detail. Numerical results can be used to validate or to modify constitutive functions depending on the stress triaxiality and the Lode parameter.

REFERENCES

[1] Bai, Y. and Wierzbicki, T. A new model of metal plasticity and fracture with pressure and Lode dependence. *Int. J. Plasticity* (2008) **24**: 1071-1096.

[2] Bao, Y. and Wierzbicki, T. On the fracture locus in the equivalent strain and stress triaxiality space. *Int. J. Mech. Sci.* (2004) **46**: 81-98.

[3] Bao, Y. and Wierzbicki, T. On the cut-off value of negative triaxiality for fracture. *Engrg. Fract. Mech.* (2005) **72**: 1049-1069.
[4] Bonora, N., Gentile, D., Pirondi, A. and Newaz, G. Ductile damage evolution under triaxial stress state: Theory and experiments. *Int. J. Plasticity* (2005) **21**: 981-1007.
[5] Brünig, M. An anisotropic ductile damage model based on irreversible thermodynamics. *Int. J. Plasticity* (2003) **19**: 1679-1713.
[6] Brünig, M. Numerical analysis of anisotropic ductile continuum damage. *Comput. Methods Appl. Mech. Engrg.* (2003) **192**: 2949-2976.
[7] Brünig, M. Albrecht, D. and Gerke, S. Numerical analysis of stress-triaxiality-dependent inelastic deformation behavior of aluminum alloys. *Int. J. Damage Mech.* (2011) **20**: 299-317.
[8] Brünig, M., Chyra, O., Albrecht, D., Driemeier, L. and Alves, M. A ductile damage criterion at various stress triaxialities. *Int. J. Plasticity* (2008) **24**: 1731-1755.
[9] Brünig, M. Gerke, S. and Hagenbrock, V. Micro-mechanical studies on the effect of stress triaxiality and the Lode parameter on ductile damage. *Int. J. Plasticity* (2013) **50**: 49-65.
[10] De Souza Neto, E.A. and Peric, D. A computational framework for a class of fully coupled models for elasto-plastic damage at finite strains with reference to the linearization aspects. *Comput. Methods Appl. Mech. Engrg.* (1996) **130**: 179-193.
[11] Driemeier, L., Brünig, M., Micheli, G. and Alves, M. Experiments on stress-triaxiality-dependence of material behavior of aluminum alloys. *Mech. Mater.* (2010) **42**: 207-217.
[12] Dunand, M. and Mohr, D. On the predictive capabilities of the shear modified Gurson and the modified Mohr-Coulomb fracture models over a wide range of stress triaxialities and Lode angles. *J. Mech. Phys. Solids* (2011) **59**: 1374-1394.
[13] Gao, X., Zhang, G. and Roe, C. A study on the effect of stress state on ductile fracture. *Int. J. Damage Mech.* (2010) **19**: 75-94.
[14] Mohr, D. and Henn, S. Calibration of stress-triaxiality dependent crack formation criteria: A new hybrid experimental-numerical method. *Exper. Mech.* (2007) **47**: 805-820.
[15] Simo, J.C. and Ju, J.W. Strain- and stress-based continuum damage models. II. Computational aspects. *Int. J. Solids Struct.* (1987) **23**: 841-869.